

SUPPLEMENTARY INFORMATION

IMAB ANTIBODY BINDS SINGLE-STRANDED CYTOSINE-RICH SEQUENCES AND UNFOLDS DNA I-MOTIFS

Joseph Boissieras,[†] Hugues Bonnet,[†] Maria Fidelia Susanto,
Dennis Gomez, Eric Defrancq, Anton Granzhan,^{*} and Jérôme Dejeu^{*}

Table of contents

Biolayer Interferometry (BLI) studies

Figure S1. BLI response during immobilization of hTeloC-27 at pH 6.0 and 7.5	S2
Figure S2. BLI sensorgrams obtained for interaction of iMab scFv-His₆-FLAG with hTeloC at pH 6.0 and pH 7.5	S2
Figure S3. BLI sensorgrams obtained for interaction of iMab with hTeloC-27 and the constrained system (1)	S2
Figures S4–S7. BLI sensorgrams obtained for interaction of iMab with various variants of hTeloC sequence	S3–S10
Figures S8–S9. BLI sensorgrams obtained for interaction of iMab with hp-ATT and ss-DNA	S11–S12
Table S1. Oligonucleotide sequences and the corresponding K_D values for the two variants of iMab at pH 6.0 and 7.5	S13
Figure S10. BLI sensorgrams obtained after dipping in ammonia solution	S14
Table S2. Kinetic and thermodynamic constants for interaction of iMab (scFv-His₆) with the different HTeloC substrates at pH 6 prior to and after dipping into ammonia solution	S15

Circular dichroism (CD) and gel electrophoresis studies

Figure S11. pH titration (A) and CD spectra of hTeloC-27 at pH 6.0, 6.5 and pH 7.5 (B)	S16
Figure S12. CD spectra of various variants of hTeloC sequence	S17
Figure S13. Native gel electrophoresis of hTeloC-2x6T and hTeloC-3x4 at different concentrations	S18

Bulk-FRET experiments

Figure S14. CD and fluorescence emission spectra of the substrates used in bulk-FRET experiments at pH 5.5 and 7.5	S19
Figure S15. Time-dependent variation of fluorescence emission spectra of Cy3-Py25/Cy5-CS after addition of recombinant hnRNP K	S19
Figure S16. Fluorescence emission spectra of Cy3-Py25 and Cy5-CS in the absence and in the presence of iMab	S20

Biolayer interferometry (BLI) studies

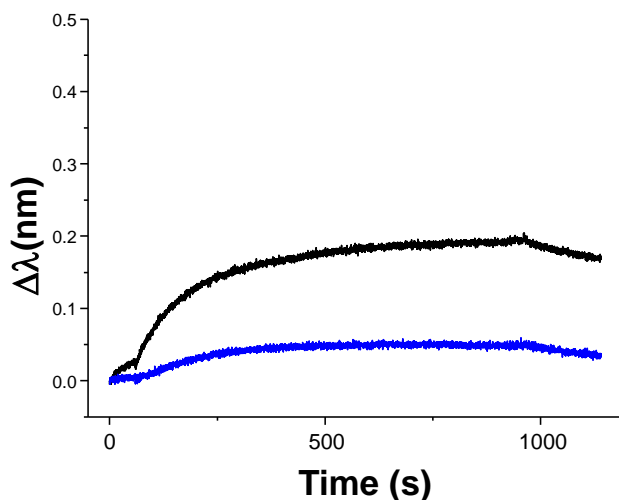


Figure S1. BLI signals observed during immobilization of hTeloC-27 at pH 6.0 (black) and 7.5 (blue).

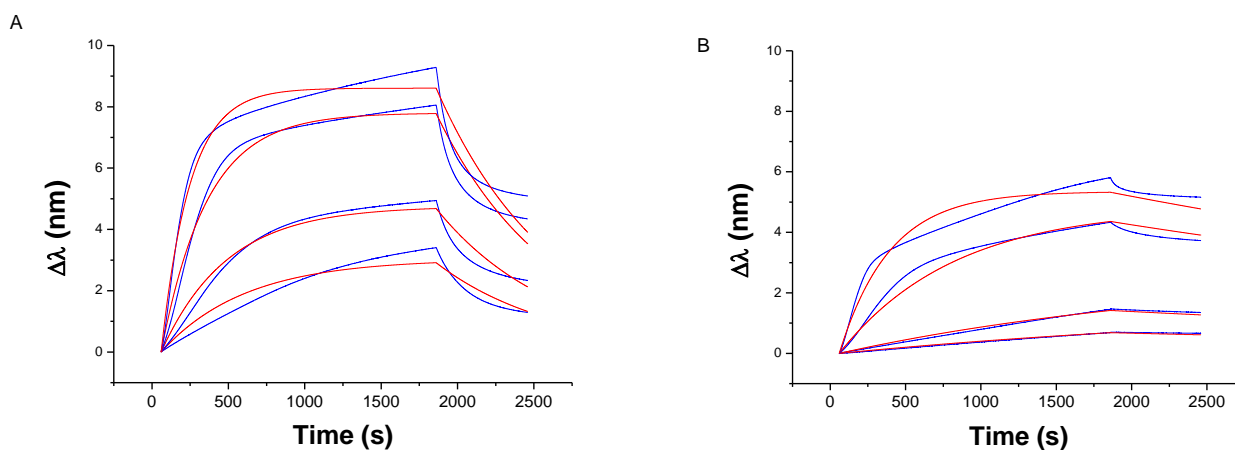


Figure S2. BLI analysis of binding of different concentrations of iMab scFv-His₆-FLAG (62.5, 125, 250 and 500 nM) to hTeloC-27 at pH 6.0 (A) and pH 7.5 (B). Blue lines are experimental curves; red lines are the fits to the 1:1 model.

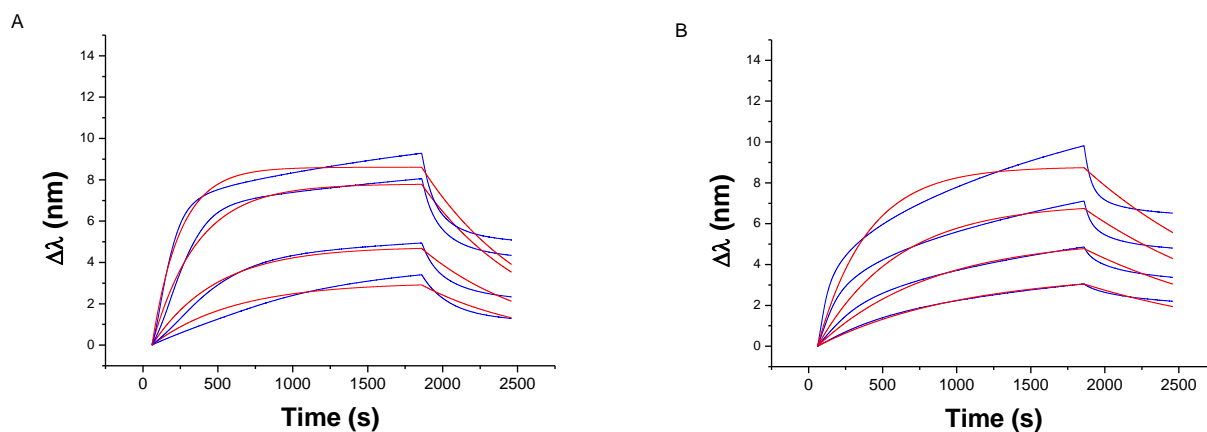
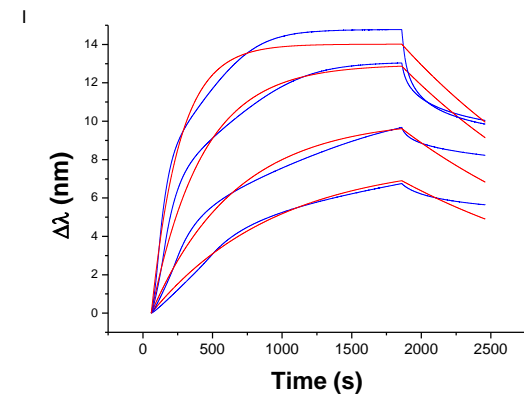
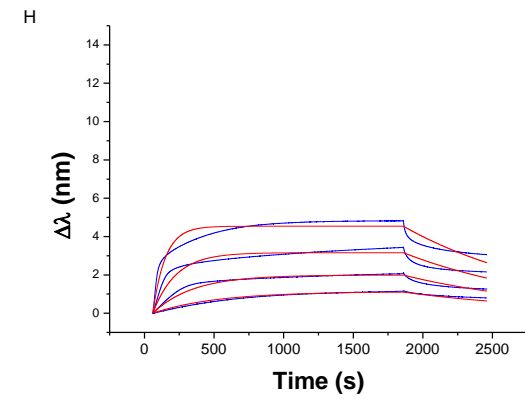
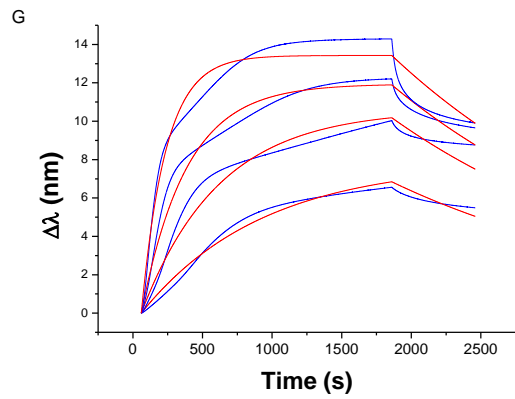
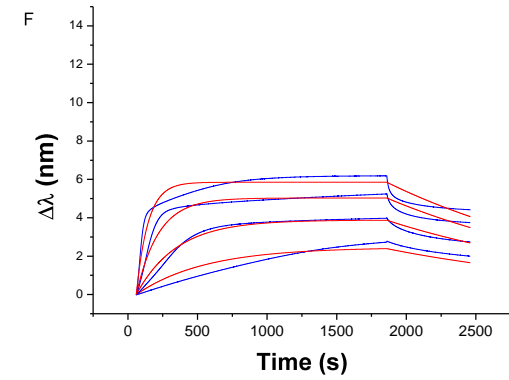
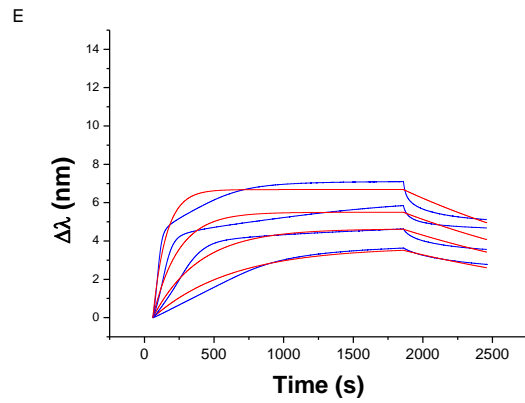
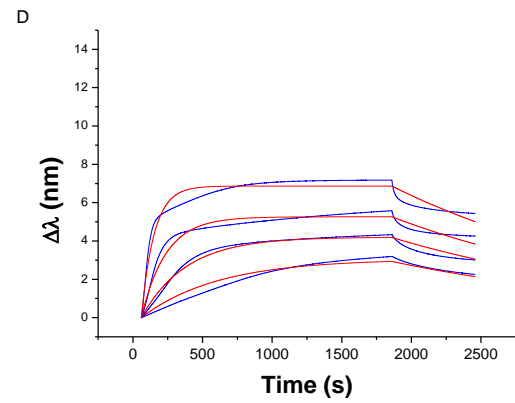
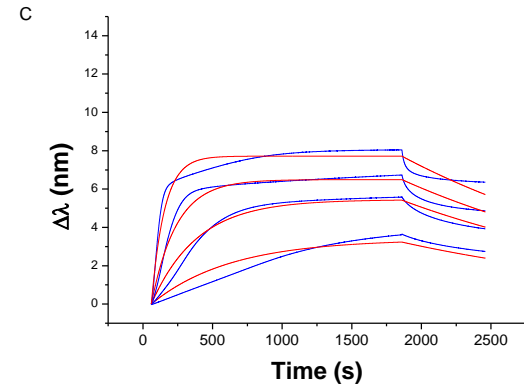
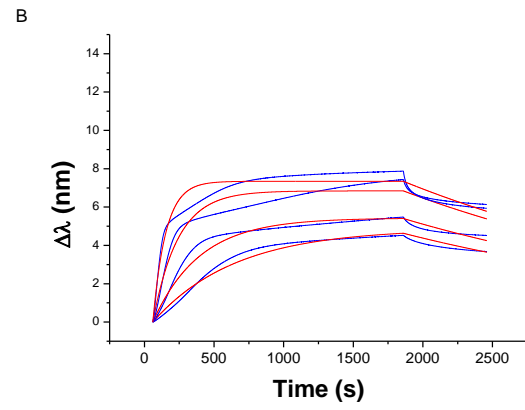
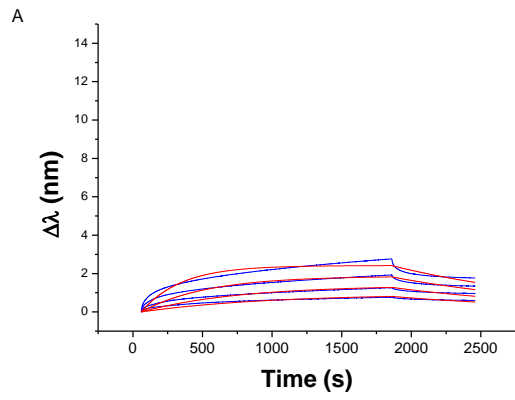


Figure S3. BLI analysis of binding of different concentrations of iMab scFv-His₆-FLAG (62.5, 125, 250 and 500 nM) to hTeloC-27 (A) and constrained hTeloC 1 (B) at pH 6.5. Blue lines are experimental curves; red lines are the fits to the 1:1 model.



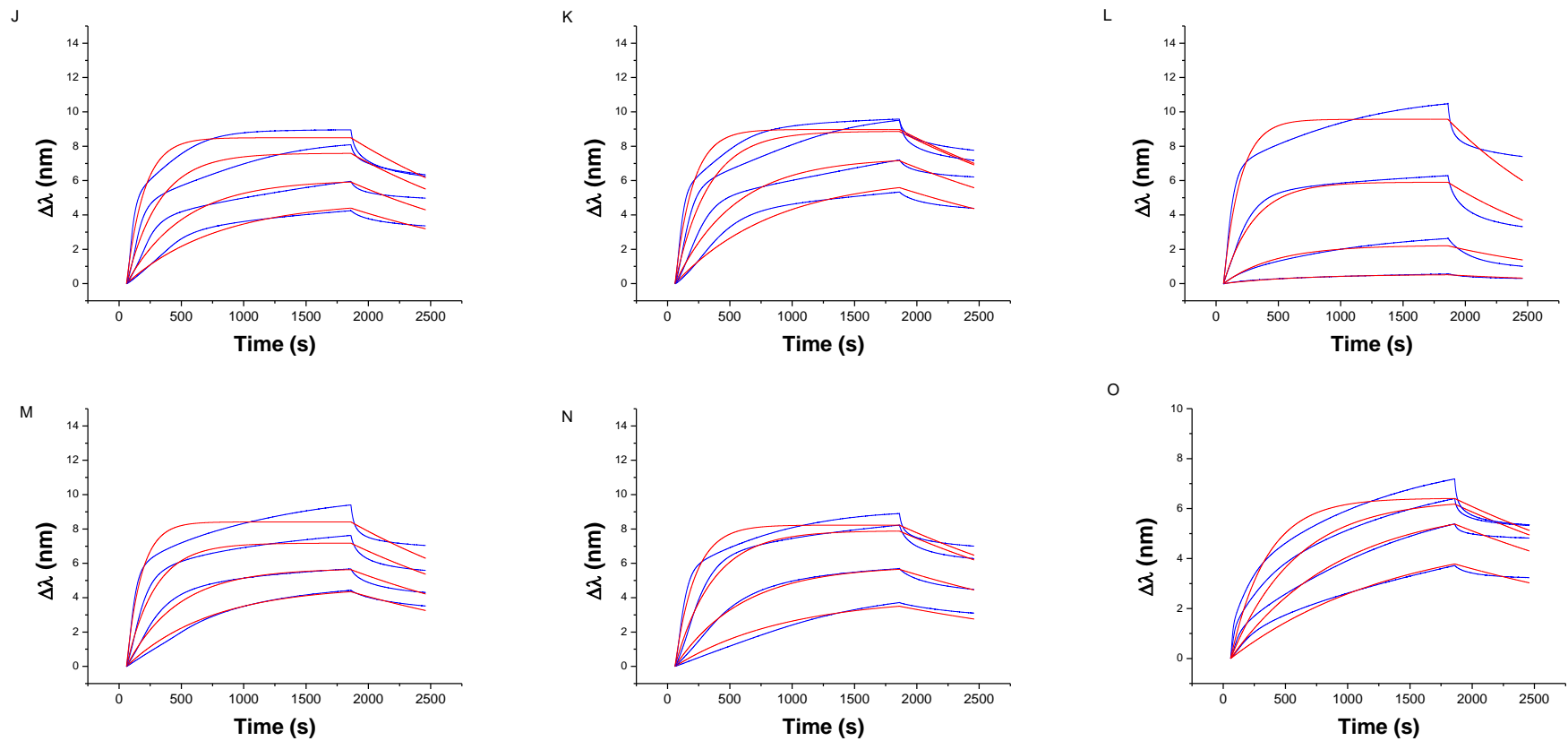
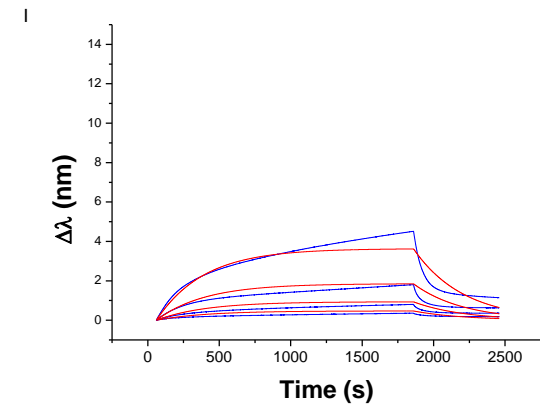
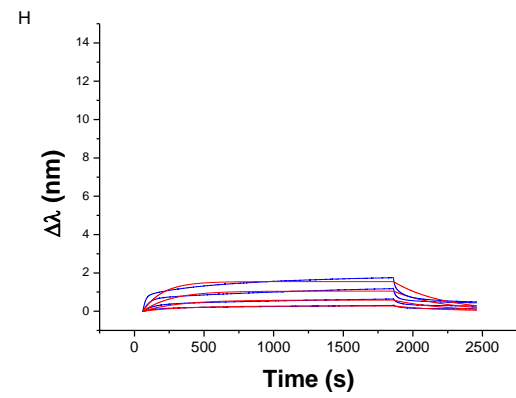
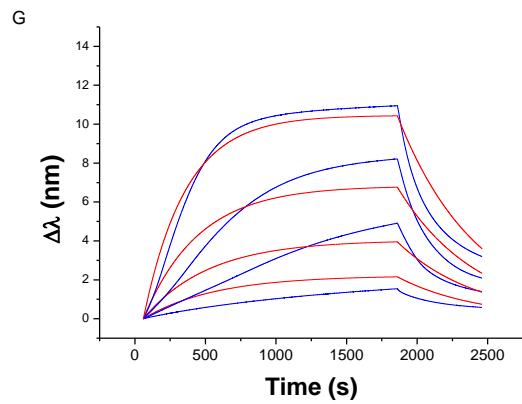
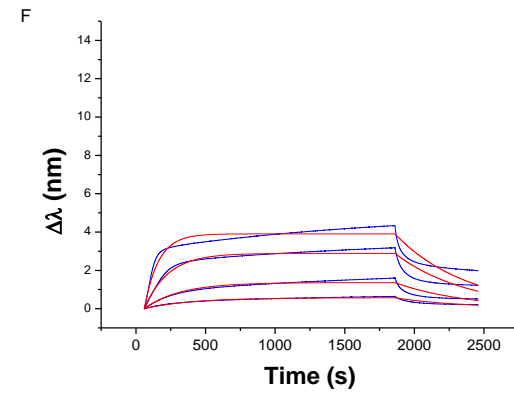
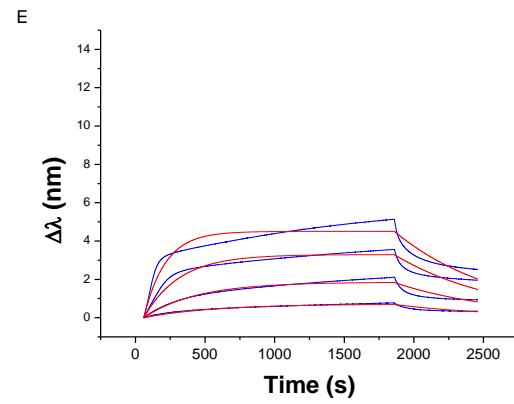
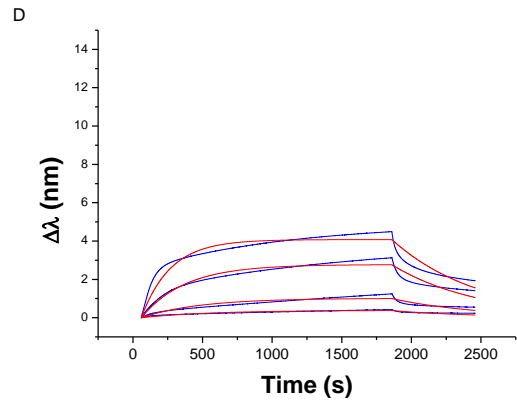
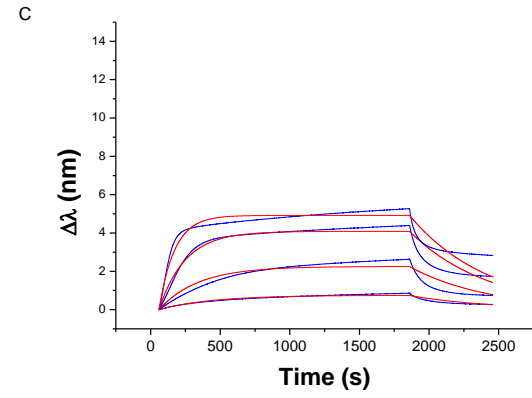
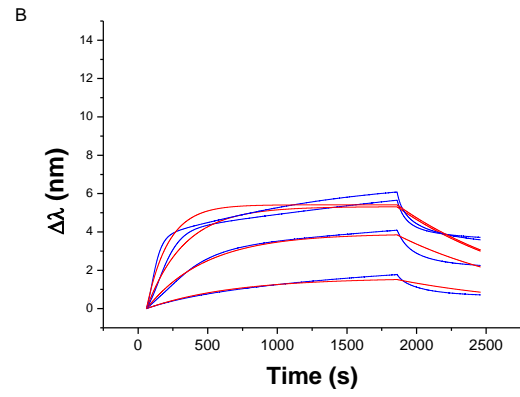
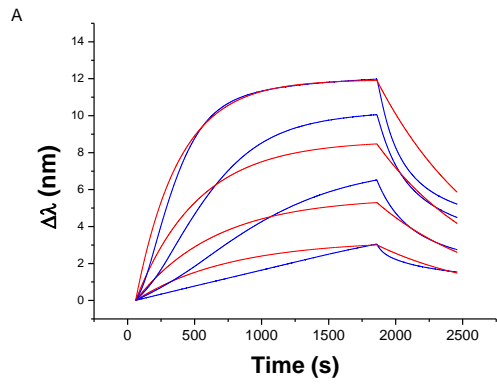


Figure S4. BLI analysis of binding of different concentrations of iMab scFv-His₆-FLAG (62.5, 125, 250 and 500 nM) to hTeloC-4x5 (**A**), hTeloC-3x4 (**B**), hTeloC 3x3 (**C**), hTeloC 3x2 (**D**), hTeloC 2x3 (**E**), hTeloC 2x3T (**F**), hTeloC-2x2 (**G**), hTeloC 1x3T (**H**), hTeloC-1x2T (**I**), hTeloC 1x6 T (**J**), hTeloC 2x6T (**K**), hTeloC-scr (**L**), hTeloC-Mut (**M**), hTeloC X3 (**N**) and hTeloC-22 (**O**) at pH 6.0. Blue lines are experimental curves; red lines are the fits to the 1:1 model.



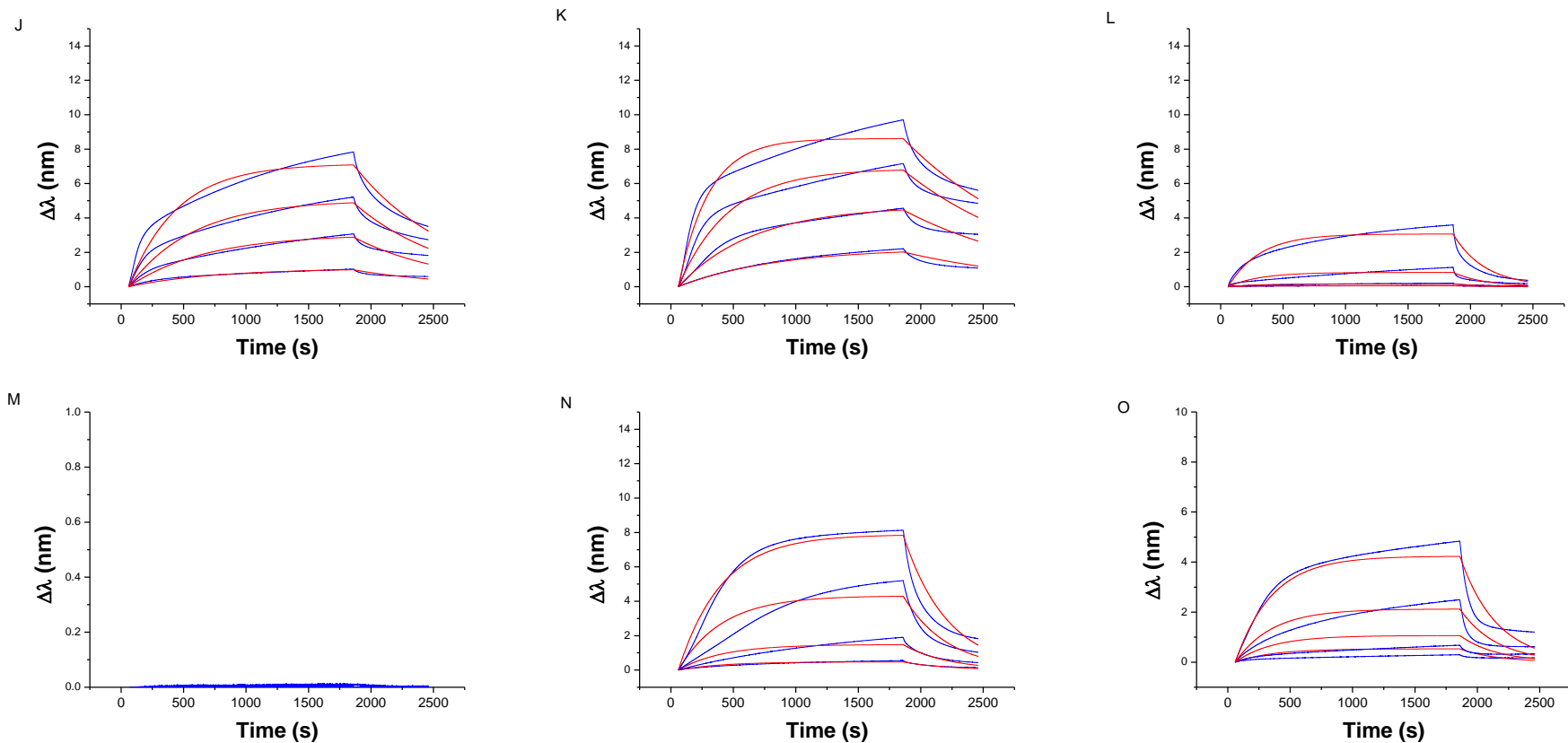
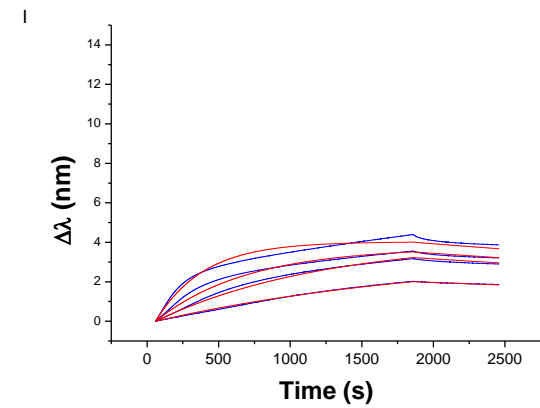
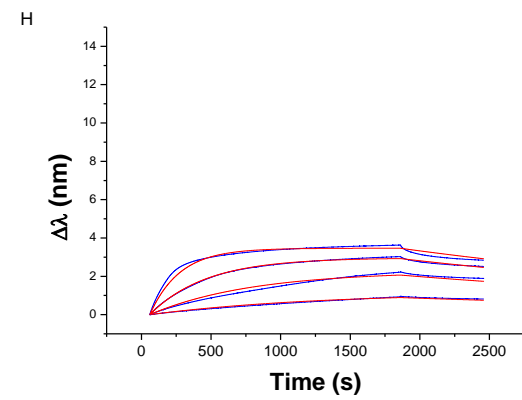
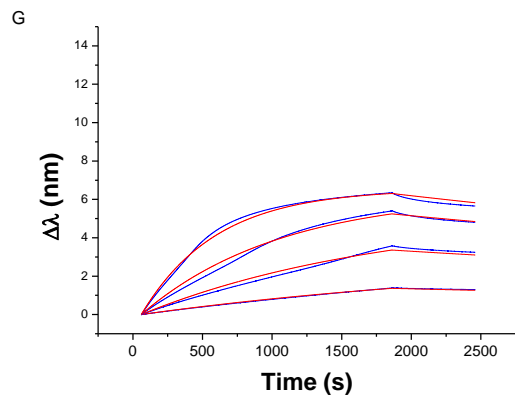
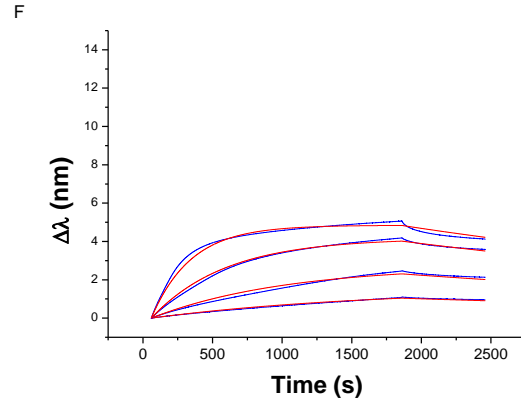
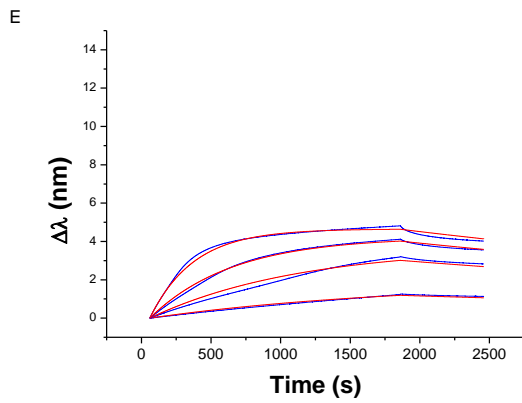
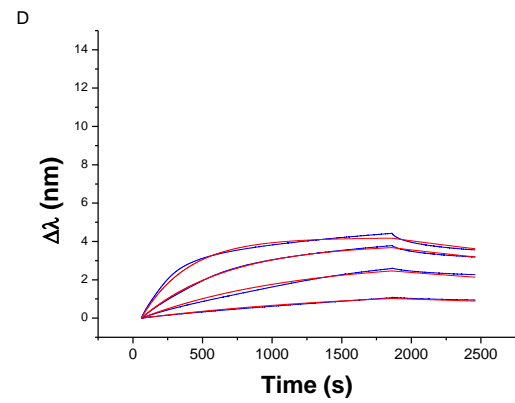
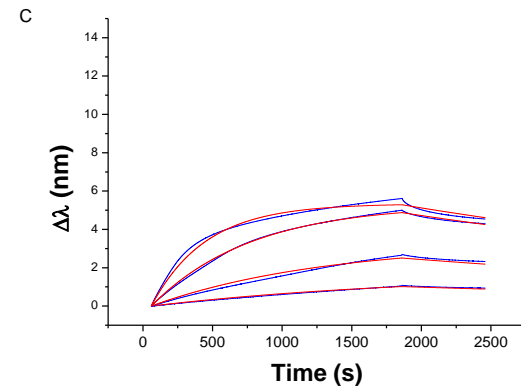
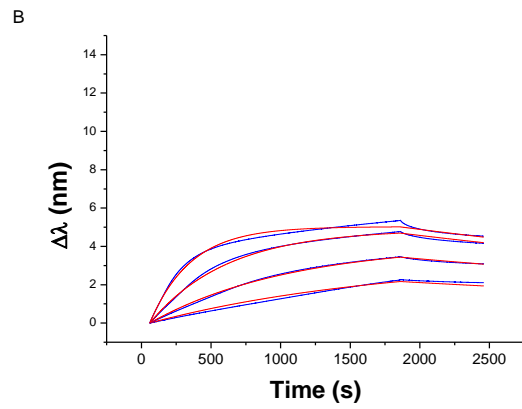
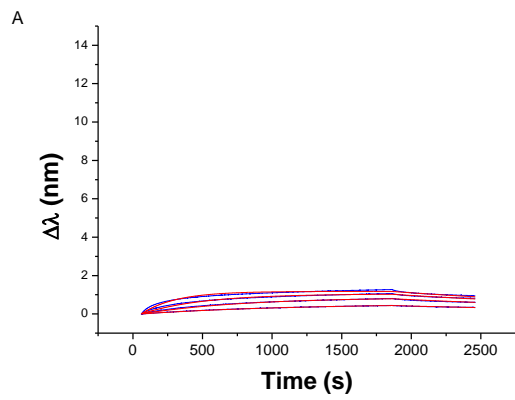


Figure S5. BLI analysis of binding of different concentrations of iMab scFv-His₆-FLAG (62.5, 125, 250 and 500 nM) to hTeloC-4x5 (**A**), hTeloC-3x4 (**B**), hTeloC 3x3 (**C**), hTeloC 3x2 (**D**), hTeloC 2x3 (**E**), hTeloC 2x3T (**F**), hTeloC-2x2 (**G**), hTeloC 1x3T (**H**), hTeloC-1x2T (**I**), hTeloC 1x6 T (**J**), hTeloC 2x6T (**K**), hTeloC-scr (**L**), hTeloC-Mut (**M**), hTeloC-X3 (**N**) and hTeloC-22 (**O**) at pH 7.5. Blue lines are experimental curves; red lines are the fits to the 1:1 model.



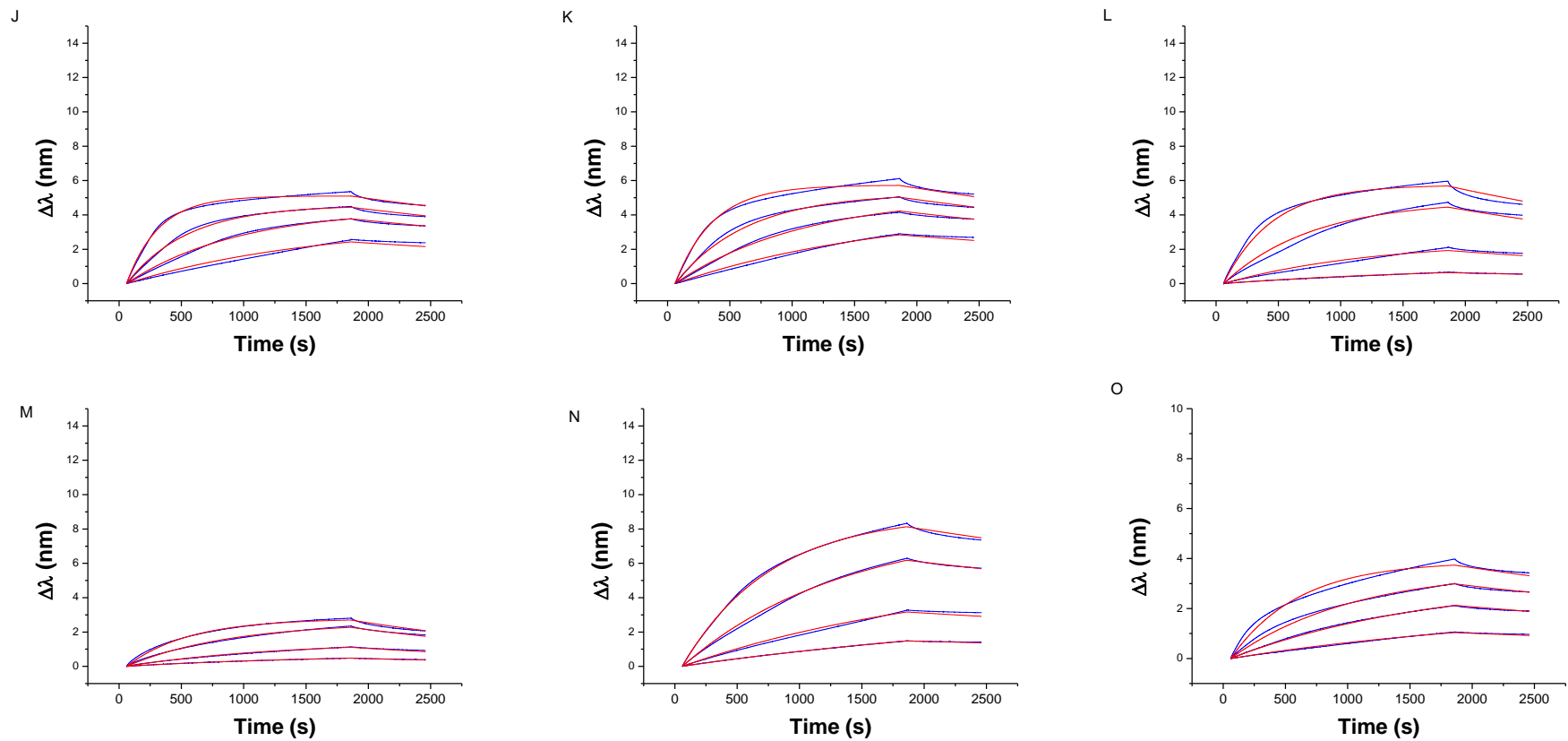
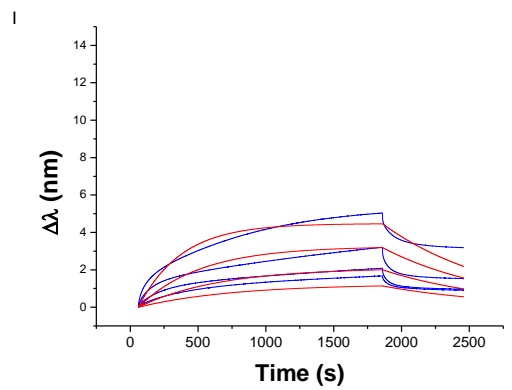
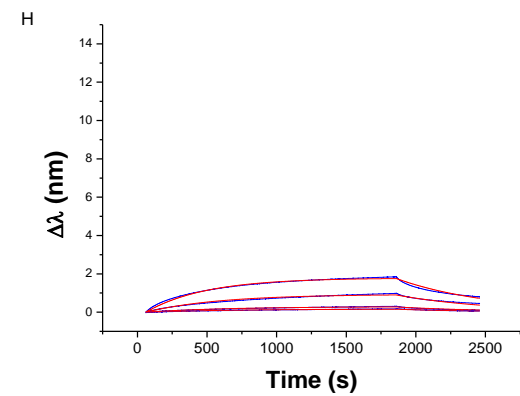
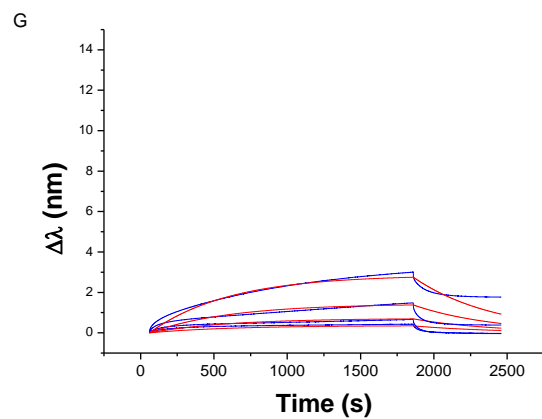
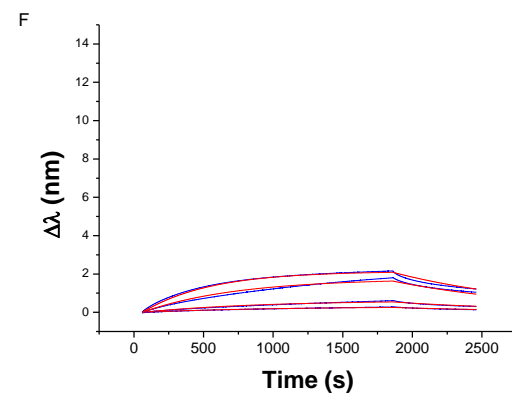
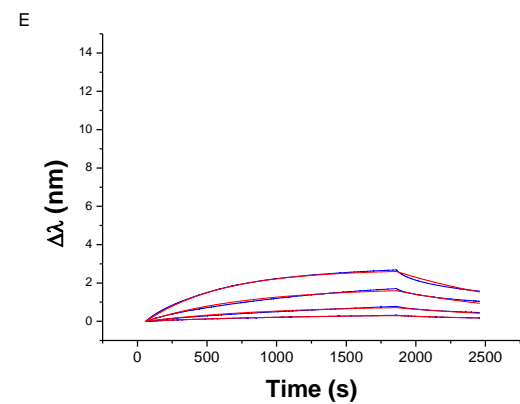
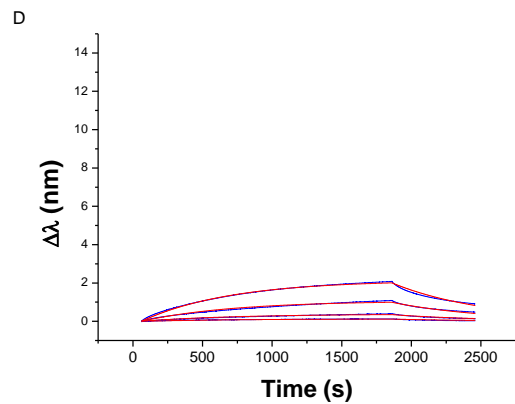
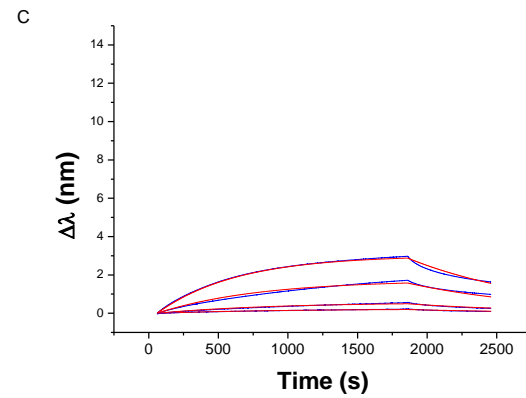
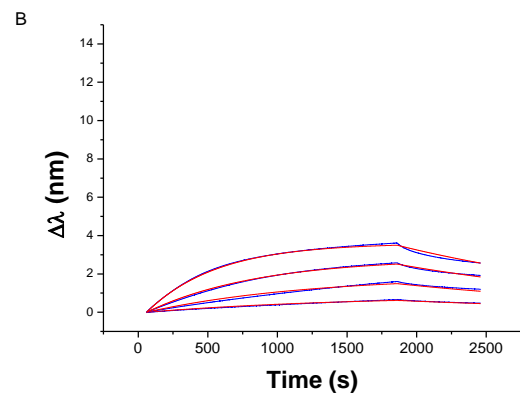
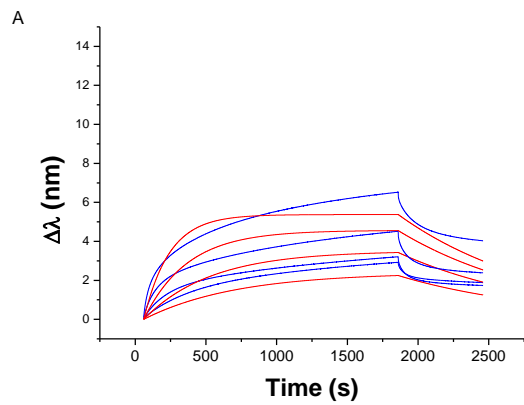


Figure S6. BLI analysis of binding of different concentrations of iMab scFv-His₆ (62.5, 125, 250 and 500 nM) to hTeloC-4x5 (**A**), hTeloC-3x4 (**B**), hTeloC 3x3 (**C**), hTeloC 3x2 (**D**), hTeloC 2x3 (**E**), hTeloC 2x3T (**F**), hTeloC-2x2 (**G**), hTeloC 1x3T (**H**), hTeloC-1x2T (**I**), hTeloC 1x6 T (**J**), hTeloC 2x6T (**K**), hTeloC-scr (**L**), hTeloC-Mut (**M**), hTeloC-X3 (**N**) and hTeloC-22 (**O**) at pH 6.0. Blue lines are experimental curves; red lines are the fits to the 1:1 model.. Blue lines are experimental curves; red lines are the fits to the 1:1 model.



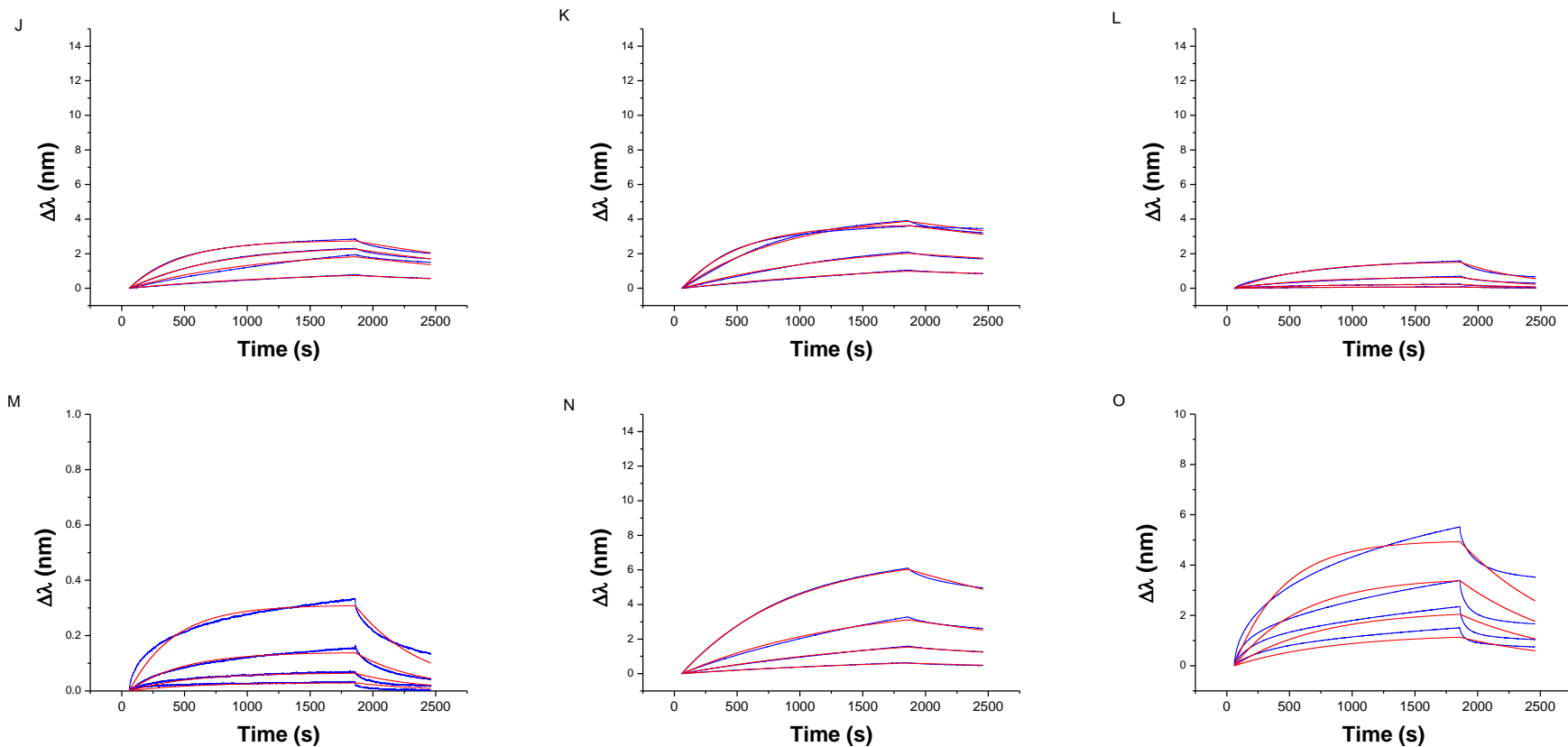


Figure S7. BLI analysis of binding of different concentrations of iMab scFv-His₆ (62.5, 125, 250 and 500 nM) to hTeloC-4x5 (**A**), hTeloC-3x4 (**B**), hTeloC 3x3 (**C**), hTeloC 3x2 (**D**), hTeloC 2x3 (**E**), hTeloC 2x3T (**F**), hTeloC-2x2 (**G**), hTeloC 1x3T (**H**), hTeloC-1x2T (**I**), hTeloC 1x6 T (**J**), hTeloC 2x6T (**K**), hTeloC-scr (**L**), hTeloC-Mut (**M**), hTeloC-X3 (**N**) and hTeloC-22 (**O**) at pH 7.5. Blue lines are experimental curves; red lines are the fits to the 1:1 model.

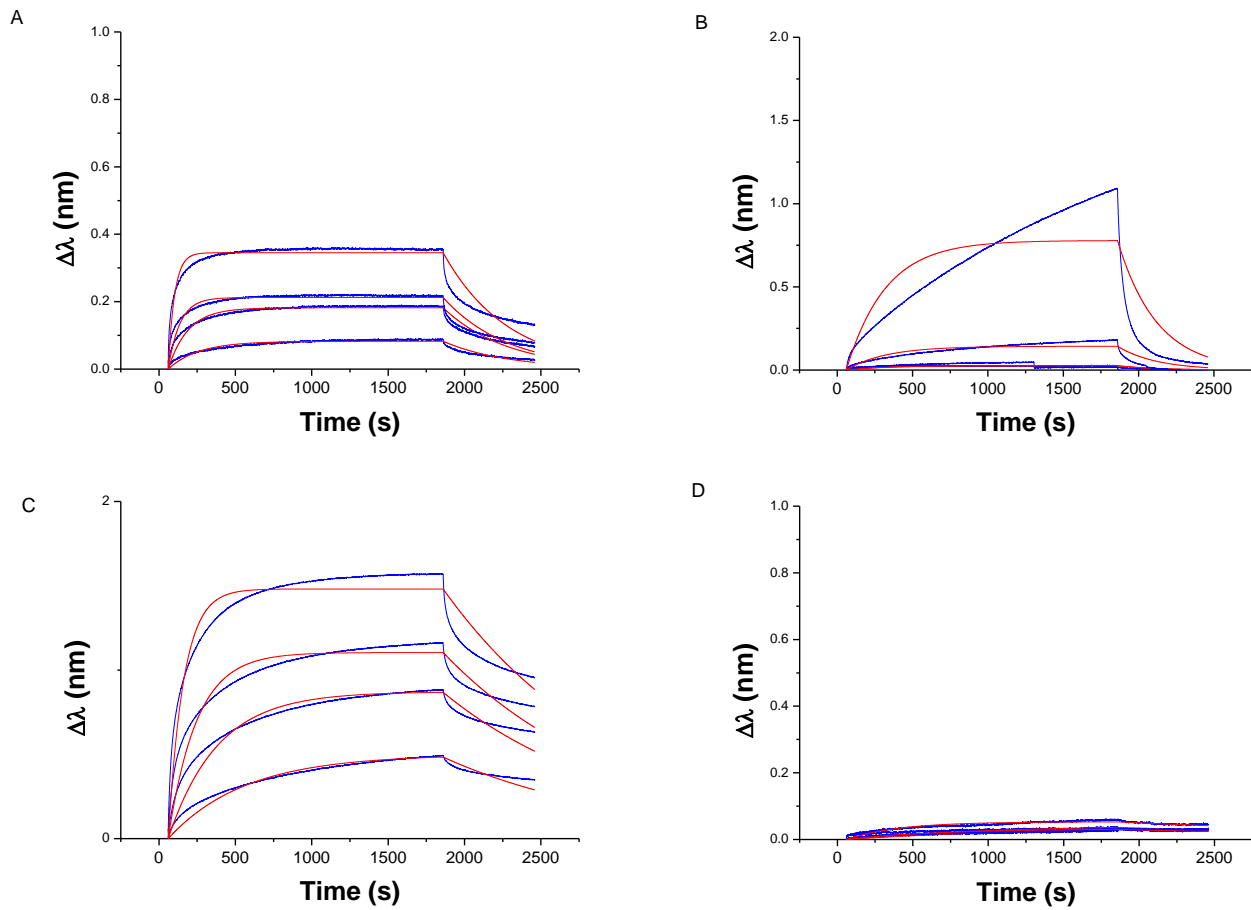


Figure S8. Bio-layer interferometry (BLI) analysis of binding of different concentrations of iMab scFv-His₆-FLAG at pH 6 (**A** and **C**) and 7.5 (**B** and **D**) for hp-ATT (**A-B**) and ss-DNA (**C-D**). The red lines are the fitting of the experiment. Concentration range: 62.5, 125, 250 and 500 nM.

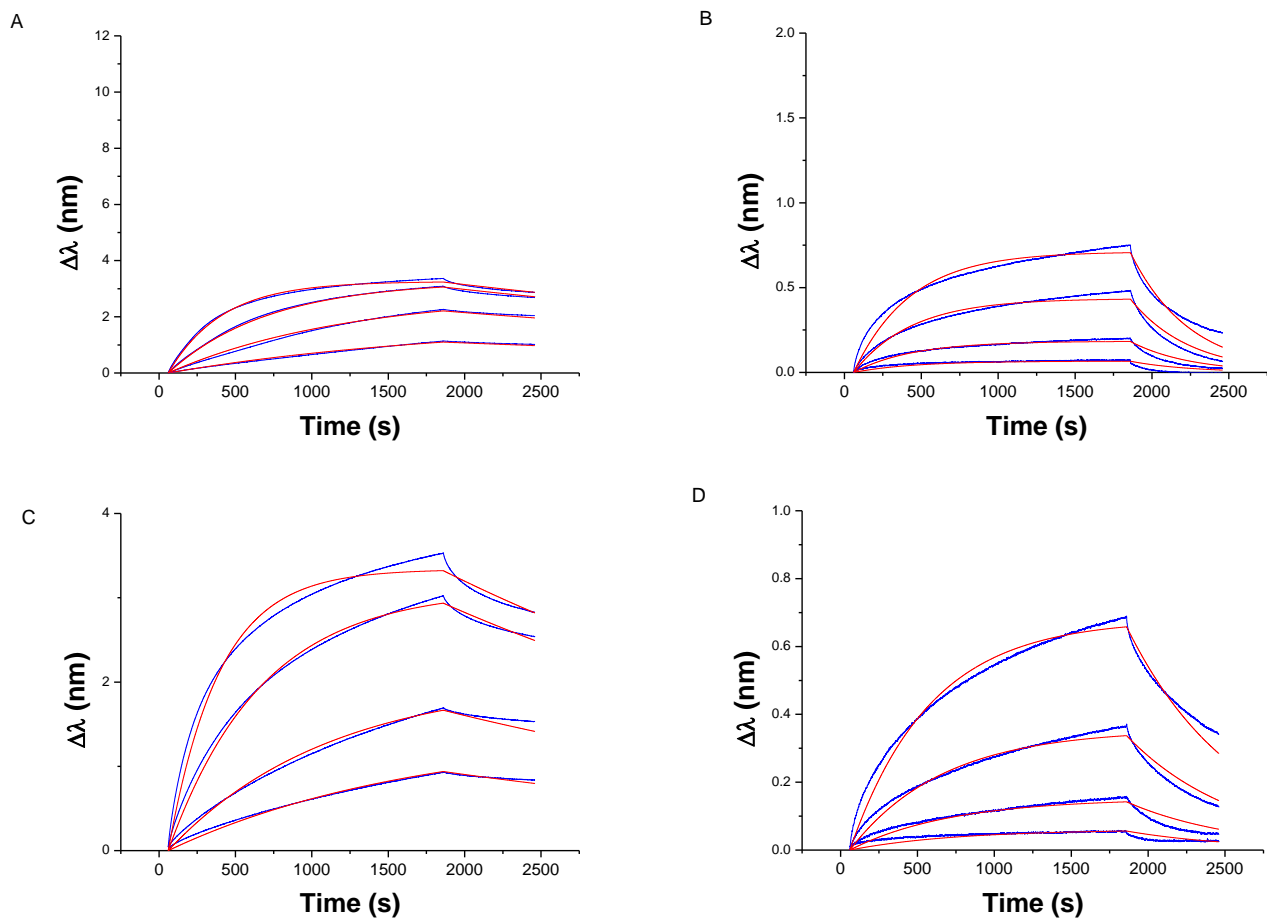


Figure S9. Bio-layer interferometry (BLI) analysis of binding of different concentrations of iMab scFv-His₆ at pH 6 (**A** and **C**) and 7.5 (**B** and **D**) for hp-ATT (**A-B**) and ss-DNA (**C-D**). The red lines are the fitting of the experiment. Concentration range: 62.5, 125, 250 and 500 nM.

Table S1. Oligonucleotide sequences used in this study and the corresponding K_D values for the two variants of iMab, obtained from BLI experiments at pH 6.0 or 7.5 and 20 °C.^a

Acronym	Sequence (5'→3')	iM folding, ^a at pH:		number of C / length (nt)	K_D at pH 6.0 (nM)		K_D at pH 7.5 (nM)	
		6.0	7.5		scFv-His ₆	scFv-His ₆ -FLAG	scFv-His ₆	scFv-His ₆ -FLAG
hTeloC-4x5	TCCCCCTCCCCCTACCCCTCCCCCTA	+	–	20 / 27	63 (50; 75)	137 (112; 162)	102 (80; 128)	22 (15; 28)
hTeloC-27	TAACCCCTAACCCCTAACCCCTAA	+	–	12 / 27	34 (24; 44)	28 (23; 31)	108 (63; 153)	91 (18; 164)
hTeloC-3x4	TAATAACCCCTAACCCCTAACCCCTAA	+	–	12 / 27	29 (17; 41)	22 (18; 26)	178 (135; 221)	138 (67; 209)
hTeloC-2x6T	TTTTAACCCCTAACCCCTAATTT	+	–	12 / 27	65 (54; 76)	31 (31; 31)	67 (48; 86)	170 (118; 222)
hTeloC-scr	TACACTCACACTCACACTCACACTCAA	–	–	12 / 27	62 (50; 74)	57 (53; 61)	n.b. ^c	n.b.
hTeloC-3x3	TAATAATAACCCCTAACCCCTAACCCCTAA	– ^d	–	9 / 27	49 (31; 67)	27 (24; 30)	716 (466; 966)	325 (205; 445)
hTeloC-3x2	TAATAACCTAACCTAACCTAATAATAA	–	–	6 / 27	43 (16; 70)	30 (25; 35)	n.b.	n.b.
hTeloC-2x3	TAATAATAACCCCTAACCCCTAATAATAA	–	–	6 / 27	32 (22; 42)	30 (24; 36)	475 (438; 512)	195 (109; 281)
hTeloC-2x3T	TTTTTTTAAACCCCTAACCCCTAATTTTTT	–	–	6 / 27	35 (27; 43)	30 (26; 34)	396 (206; 586)	241 (148; 334)
hTeloC-1x6T	TTTTTTTTTAAACCCCTAATTTTTTTT	–	–	6 / 27	27 (23; 31)	47 (38; 56)	125 (113; 137)	493 (468; 518)
hTeloC-2x2	TAATAACCTAATCTAACCTAATAATAA	–	–	5 / 27	40 (30; 50)	50 (35; 65)	n.b. ^c	58 (40; 76)
hTeloC-1x3T	TTTTTTTTTTTAAACCCCTAATTTTTTTTTT	–	–	3 / 27	33 (25; 41)	60 (38; 82)	891 (408; 1374)	346 (338; 354)
hTeloC-1x2T	TTTTTTTTTTTAAACCTAATTTTTTTTTT	–	–	2 / 27	26 (12; 40)	65 (43; 87)	303 (252; 354)	108 (62; 154)
hTeloC-22	CCCTAACCCCTAACCCCTAACCCCT	+	–	12 / 22	62 (58; 66)	61 (55; 66)	250 (100; 400)	45 (10; 80)
hTeloC-mut	CGGTAACGGTAACGGTAACGGT	–	–	4 / 22	141 (117; 165)	169 (102; 236)	n.b. ^c	n.b.
hTeloC-X3	CCCTAACCCCTAACCCCTAA	– ^d	–	9 / 18	54 (35; 73)	20 (8; 32)	215 (170; 260)	396 (272; 520)
hp-ATT	GCGCGCGCATTGCGCGCGC	–	–	8 / 19	38 (23; 53)	26 (8; 44)	n.b.	n.b.
ss-DNA	GGCATAGTGCGTGGGCG	–	–	3 / 17	50 (27; 73)	43 (24; 62)	n.b.	n.b.

^a Data are means \pm s.d. from $N = 2$ independent measurements. ^b according to CD spectra (cf. [Supplementary Figure S12](#)). ^c n.b. = Not determined, due to weak BLI signals (no binding) or uncoherent value obtained during the fitting (R_{\max} too high). ^d partial iM formation was observed at pH 5.5.

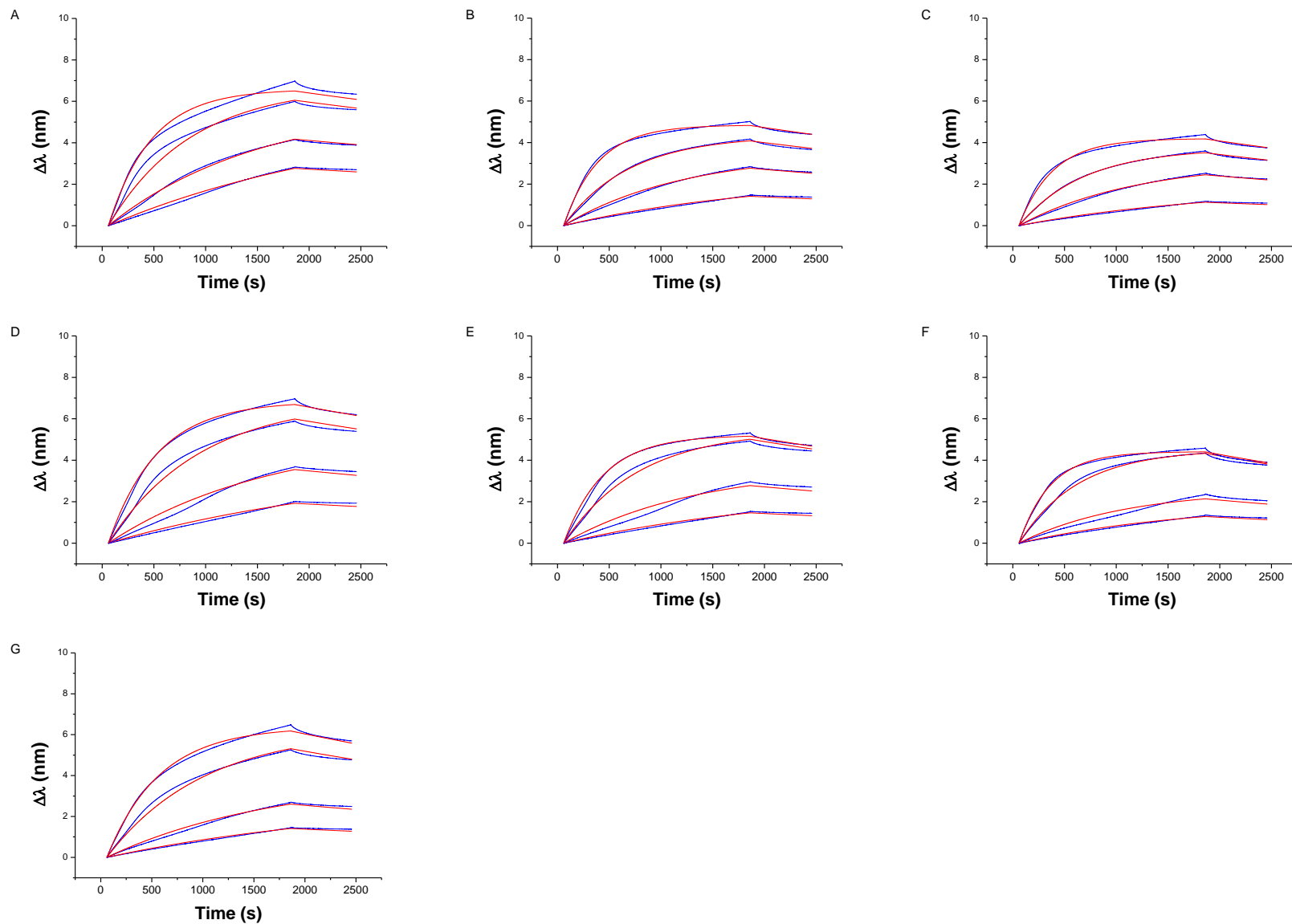


Figure S10. BLI analysis of binding of different concentrations of iMab scFv-His₆ (62.5, 125, 250 and 500 nM) to hTeloC-27 (A), hTeloC-3x4 (B), hTeloC 2x6T (C), hTeloC 3x4 (D), hTeloC 2x3 (E), hTeloC 1x3T (F), hTeloC X3 (G) at pH 6 after dipping of the immobilized structured on ammoniac solution at pH 10, 50°C during 10 minutes. Blue lines are experimental curves; red lines are the fits to the 1:1 model.

Table S2. Kinetic constants (k_{on} and k_{off}) and calculated dissociation equilibrium constants (K_D) for interaction of iMab (scFv-His₆) with several HTeloC substrates at pH 6 and 20 °C, prior to and after dipping in NH₃ solution (pH 10, 50 °C during 10 min).^a

Substrate	pH 6.0 (prior to dipping in NH ₃ solution)			pH 6.0 (after dipping in NH ₃ solution)		
	k_{on} (10 ³ M ⁻¹ s ⁻¹)	k_{off} (10 ⁻⁴ s ⁻¹)	K_D (nM)	k_{on} (10 ³ M ⁻¹ s ⁻¹)	k_{off} (10 ⁻⁴ s ⁻¹)	K_D (nM)
hTeloC-27	2.7; 4.5	1.1; 1.2	24; 44	4.1; 5.1	0.5; 1.6	12; 36
hTeloC-3x4	5.9; 7.0	1.2; 2.4	17; 41	5.0; 6.4	0.9; 2.1	18; 32
hTeloC-2x6T	2.8; 3.6	1.5; 2.7	54; 76	5.1; 6.5	1.1; 2.4	21; 37
hTeloC-X3	2.0; 2.9	0.7; 2.2	35; 73	2.9; 4.1	1.1; 2.2	38; 54
hTeloC-3x3	4.0; 4.9	1.2; 3.3	31; 67	3.6; 4.1	0.9; 2.0	25; 54
hTeloC-2x3	5.2; 6.7	1.5; 2.2	22; 42	4.2; 5.3	1.1; 2.1	26; 40
hTeloC-1x3T	8.6; 9.1	2.2; 3.7	25; 41	5.8; 6.5	1.7; 2.5	26; 43

^a Data are individual values obtained from two independent measurements.

Circular dichroism (CD) and gel electrophoresis studies

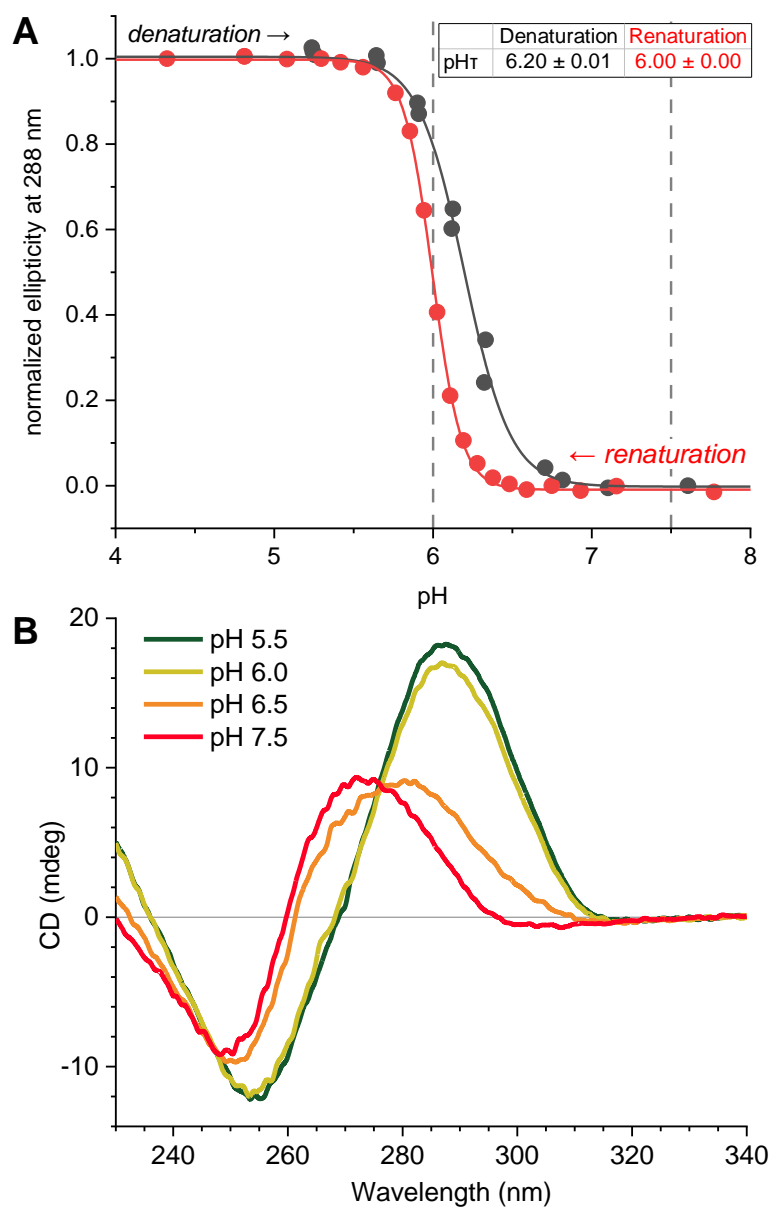


Figure S11. (A) pH-dependent denaturation/renaturation curves of hTeloC-27 (2.5 μ M in 10 mM lithium cacodylate, 100 mM potassium chloride buffer). Titrations were performed as described elsewhere (Boissieras and Granzhan, *Methods Enzymol.* 2024, 695, 233–254). Dashed lines indicate the two conditions (pH 6.0 and 7.5) used in BLI experiments. (B) CD spectra of hTeloC-27 (2.5 μ M) at pH 5.5, 6.0, 6.5 and 7.5.

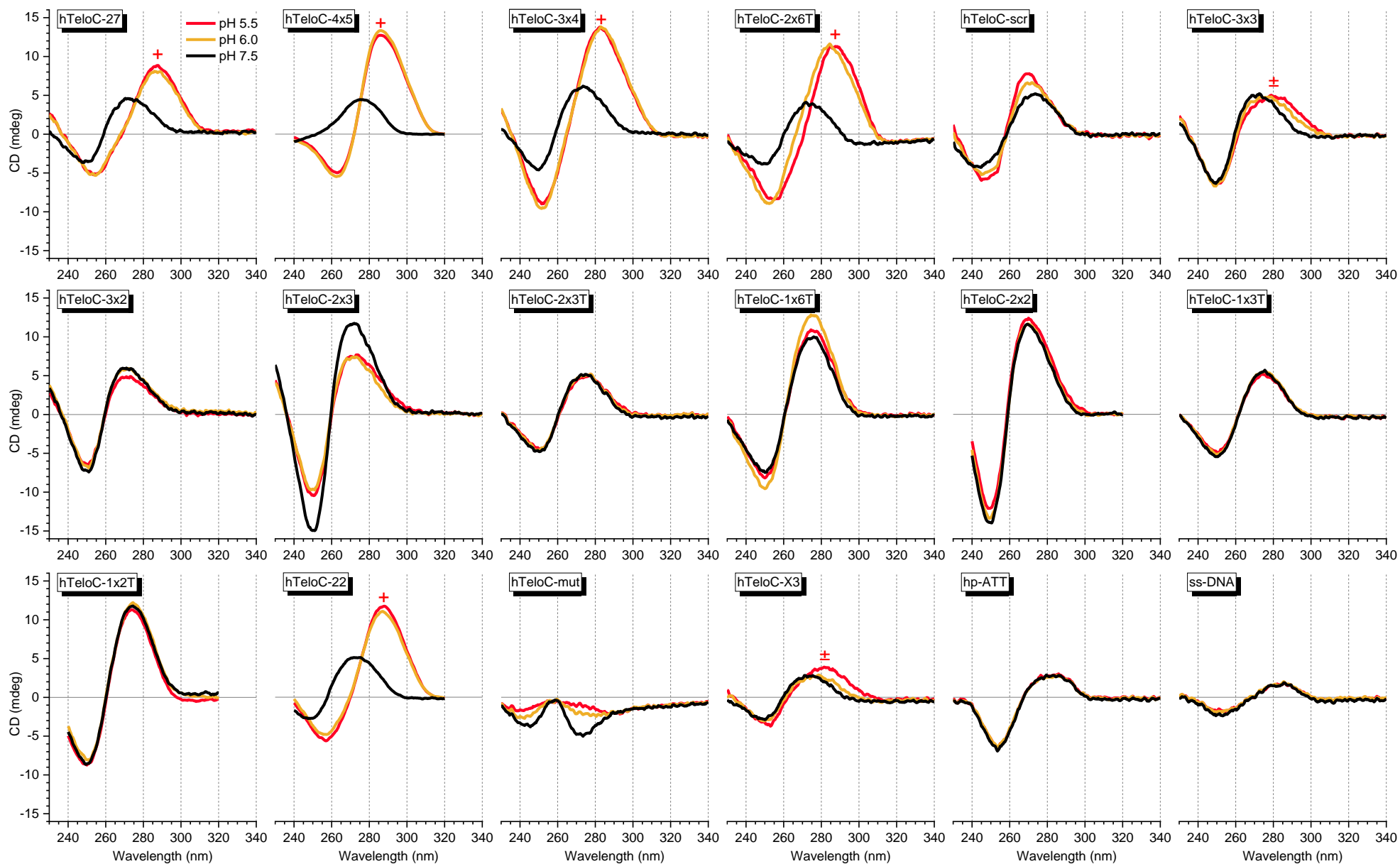


Figure S12. CD spectra of the sequences used in this study, obtained at pH 5.5 (red), 6.0 (dark yellow) and 7.5 (black). Oligonucleotide concentration $c = 2.5 \mu\text{M}$ in all cases. iM-characteristic peaks are labelled with a plus (+) symbol; peaks suggesting partial formation of iMs are labelled with a plus-minus symbol (\pm). Note that the peculiar shape of hTeloC-mut spectrum is in agreement with literature data (M. Zeraati *et al.*, *Nature Chem.* **2018**, *10*, 631–637).

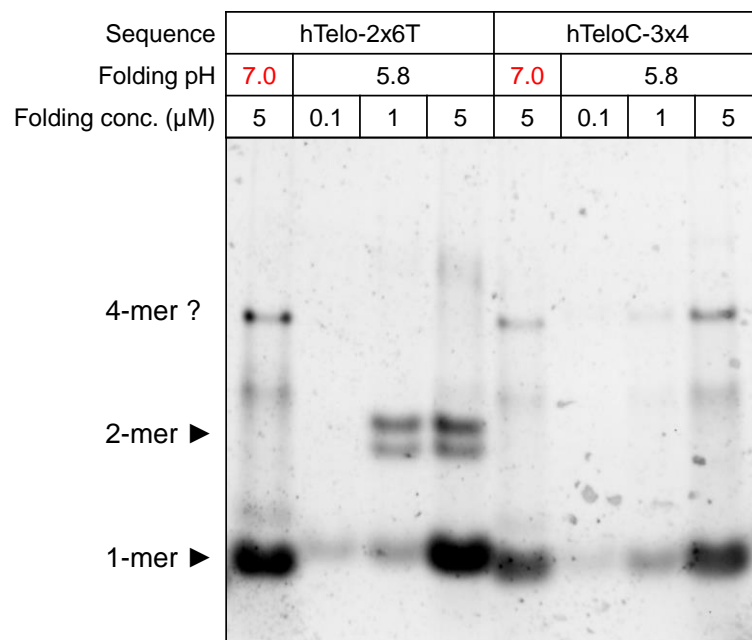


Figure S13. Native gel electrophoresis of hTeloC-2x6T and hTeloC-3x4. Oligonucleotides samples (10 μ L each) were annealed at indicated concentrations for 10 min at 95 °C and then cooled overnight in Tris-AcOH, pH 5.8 or 7.0 (control), supplemented with 2 μ L of a 6X Ficoll-based loading buffer and migrated on a 20% acrylamide gel with TAE buffer adjusted to pH 5.8, overnight at 4 °C. DNA bands were observed after a 15-min incubation in a 1:100 SYBR Green/TAE mixture in a BioRad GelDoc XR device.

Bulk-FRET experiments

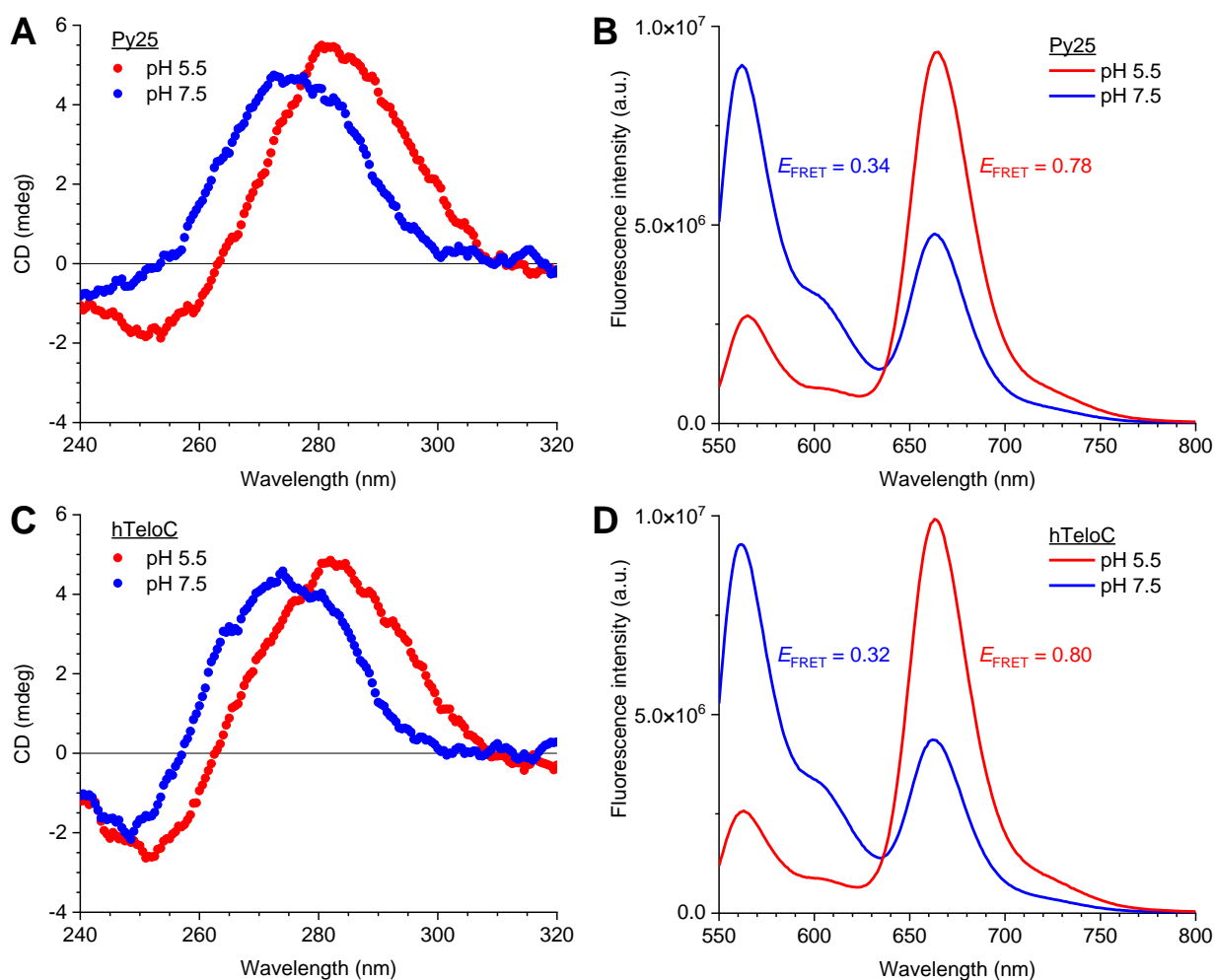


Figure S14. Circular dichroism (A, C) and fluorescence emission spectra (B, D) of Cy3-Py25/Cy5-CS (panels A–B) and Cy3-hTeloC/Cy5-CS (panels C–D) substrates (0.5 μM in bulk-FRET buffer), both recorded at pH 5.5 (red dots and lines) and pH 7.5 (blue dots and lines).

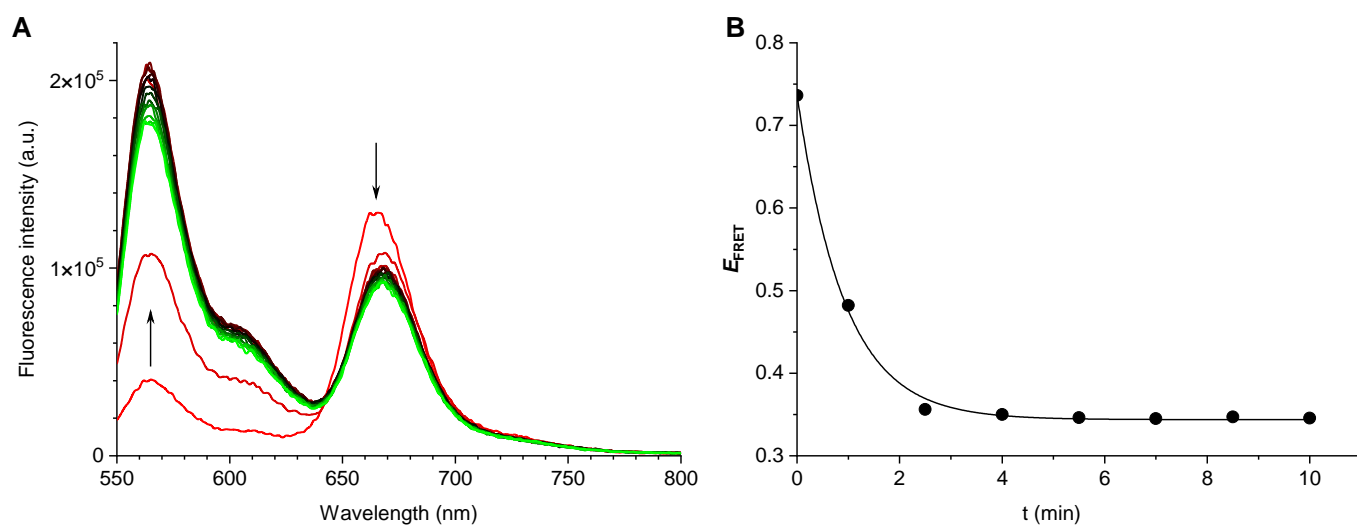


Figure S15. Time-dependent variation of fluorescence emission spectra (A) and E_{FRET} value (B) of Cy3-Py25/Cy5-CS substrate (4 nM) after addition of recombinant hnRNP K (800 nM) at pH 5.8. Spectra were recorded in ~2-min intervals.

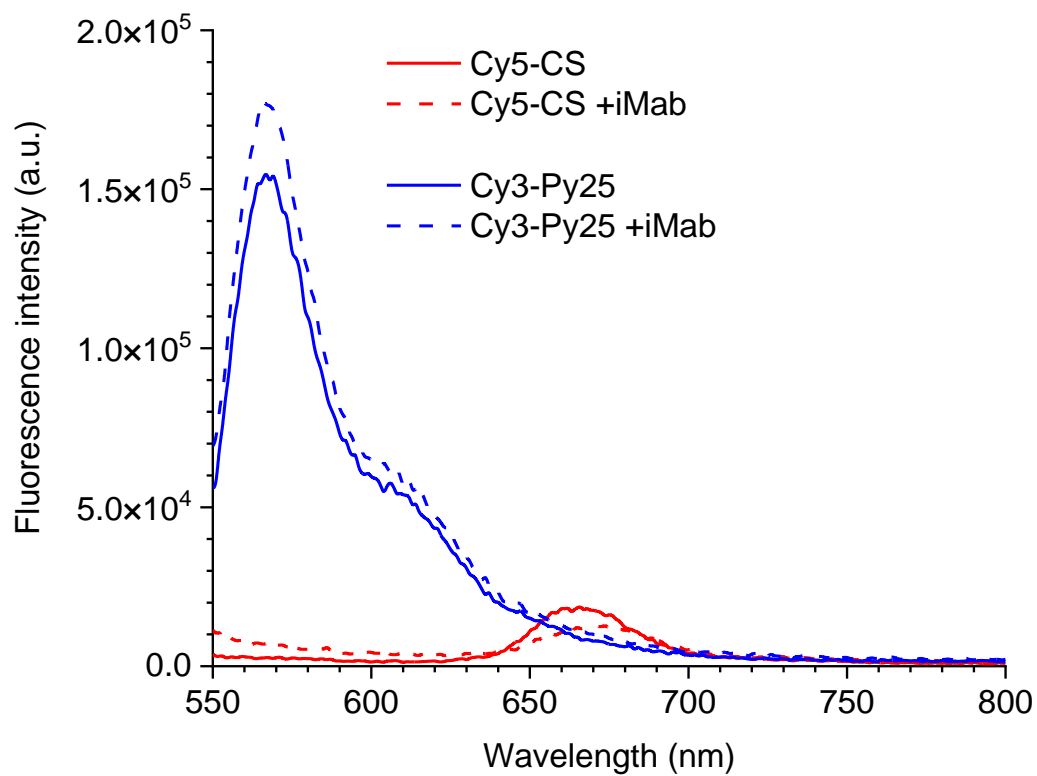


Figure S16. Fluorescence emission spectra of Cy3-Py25 (blue) and Cy5-CS (red) strands (4 nM in bulk-FRET buffer, pH 5.8), in the absence (solid lines) and in the presence of 800 nM of iMab (dashed lines). No additional changes were observed after ~1 hour of incubation time.